Research Article

Saba I. Jawad and Mustafa H. Omar*

# Experimental investigation on the influence of partially stabilised nano-$ZrO_2$ on the properties of prepared clay-based refractory mortar

https://doi.org/10.1515/jmbm-2022-0265
received May 25, 2022; accepted October 13, 2022

**Abstract:** Buildings subjected to elevated temperatures or thermal shock can be exposed to many changes in their properties, such as phase transformation and weight loss; therefore, the thermomechanical stability of mortars is essential to maintain their properties. In this work, different ratios of partially stabilised nano-zirconium oxide ($ZrO_2$) were used as a partial replacement by weight of kaolin to prepare a refractory mortar. Five ratios (5, 7.5, 10, 12.5, and 15%) of $ZrO_2$, as well as unfired kaolin, water, and internal lubricant (potassium silicate) were applied to increase the specimen's cohesion. The results showed that $ZrO_2$ additives are suitable to be used for the production of refractory mortar as a result of increased physical and mechanical strength.

**Keywords:** kaolin, mullite, nanomaterials, refractory mortar, thermomechanical properties, zirconium oxide

## 1 Introduction

Clay minerals are of interest because they are primary and secondary materials for many industries, including refractory manufacturing, which enter into many fields such as petrochemical, glass, cement, building blocks, firebricks, electrical and thermal insulation, and others [1]. Refractories properties determination depends on the used raw material and the quality control of the production technology and its ability to withstand the operational conditions to ensure the durability of the product [2]. Most of the clay used in the refractory industry contains kaolinite as a base mineral in its pseudo-hexagonal crystalline clay structure. The basic kaolinite elements are $H_2O$ (14%), $Al_2O_3$ (39.5%), and $SiO_2$ (46.5%). However, these ratios are rarely found in nature, as they contain some impurities and molten materials, which in turn negatively affect properties and limit their use [3]. The reports of the Iraqi General Establishment for Geological Survey and Mining indicated that Iraqi Kaolin contains alumina (39.5%), silica (46.5%), and water (14%) [4,5].

The weak bonding of the kaolin layers makes the clay minerals with thin and wide layers, and when water is added to the kaolin ore, the plates slide easily over each other, which gives the clay the property of plasticity to be easy to form, so kaolin is used as a binder in the manufacture of refractories [6]. When kaolin is fired at a high temperature, it is transformed into metakaolin at a temperature of (450°C). The transformation is accompanied by the destruction of the crystal structure, and when the firing process continues, the metakaolin turns into the mullite phase at a temperature of (1,400–925)°C. The transformation is accompanied by the formation of cristobalite as well [7].

The choice of the best refractory raw material is achieved by finding good and suitable characteristics for each industry to ensure its ability to withstand operational conditions [8]. Therefore, in this research, zirconium oxide (Zirconia) was selected to be added to kaolin. Zirconia has a unique set of properties such as high durability, high melting point, very low wettability, chemically inert, and high chemical resistance, so it has entered into many ordinary and advanced applications [9,10]. Zirconia is added to refractories to improve their mechanical and thermal properties [11,12].

Many previous research articles studied the refractory mortar and its properties: In 2021, Adrian *et al.* used mullite zirconia composites as bonding for refractory bricks and studied their microstructures, mineralogy, and properties by controlling the secondary oxides. The findings revealed that the composites are extremely sensitive to

*** Corresponding author: Mustafa H. Omar,** Department of Civil Engineering, Bilad Alrafidain University College, Diyala, 32001, Iraq, e-mail: Mustafahassan550@gmail.com
**Saba I. Jawad:** Department of Civil Engineering, Bilad Alrafidain University College, Diyala, 32001, Iraq

sodium oxide, which significantly harmed the microstructure, while the additions of titanium oxide and phosphorus pentoxide allow complete zircon decomposition at 1,550°C while maintaining the required green body strength [13]. In 2020, Jérôme *et al.* measured the ultimate compressive and shear stresses using slant shear tests, and temperature-dependent factors of the Mohr–Coulomb failure criterion applied to two brick/mortar combinations at temperatures ranging from room temperature to 1,450°C. The results showed that the failure can occur in the mortar and the strength decreased at 900°C [14]. In 2020, Mehmet *et al.* evaluated the effects of cement-replacing kaolin and calcined kaolin at rates of (0, 5, 10, 15, and 20%) on the toughness and mechanical properties of self-compacting mortars from room temperatures up to 900°C. The results showed an improvement in flowability of fresh mixes with inclusion rates of Kaolin and calcined Kaolin, also the strength decreased with increasing kaolin and calcined kaolin ratios at high temperatures [15].

## 2 Experimental work

This work includes preparing a refractory mortar using fired Iraqi kaolin clay with the addition of a small amount of unfired kaolin due to the high thermal and mechanical properties that fired kaolin possesses compared to the raw material before firing. The kaolin rocks were sintered at 1,200°C. Figure 1 shows the schematic representation of the experimental work. An electrical crusher was used for crushing the rocks and then sieved to different particle sizes. The particle size was determined experimentally to accomplish the best characteristics and to prevent the formation of cracks. Zirconia, which provides partially stabilised micro–nanoparticles, was used as an additive in 5, 7.5, 10, 12.5, and 15% of kaolin weight [16]. The mixture is illustrated in Table 1. First, kaolin and $ZrO_2$ were dry mixed. Then, water and potassium silicate (density of 1.25 g/cm$^3$) were added as a binder to the mixture. The hand moulding method was used to prepare the specimens. Standard ASTM F1097-91 was used to prepare cylindrical specimens with a diameter and height of 10 mm × 20 mm, respectively, by pressing the paste in an oiled mould, left to dry in the air for 1 day, and then fired at 1,200°C for 1 h with a heating rate of 4°C/min as illustrated in Figure 2. Table 2 and Figure 3 present the chemical analysis and X-ray diffraction (XRD) results of Iraqi kaolin rocks utilised in this study [17].

**Table 1:** Proportions of raw materials utilised in the mix

| Mix. | Fired kaolin (%) | Kaolin (%) | Fired additives (%) |
|---|---|---|---|
| 1 | 90 | 10 | 0 |
| 2 | 85 | 10 | 5 |
| 3 | 82.5 | 10 | 7.5 |
| 4 | 80 | 10 | 10 |
| 5 | 77.5 | 10 | 12.5 |
| 6 | 75 | 10 | 15 |

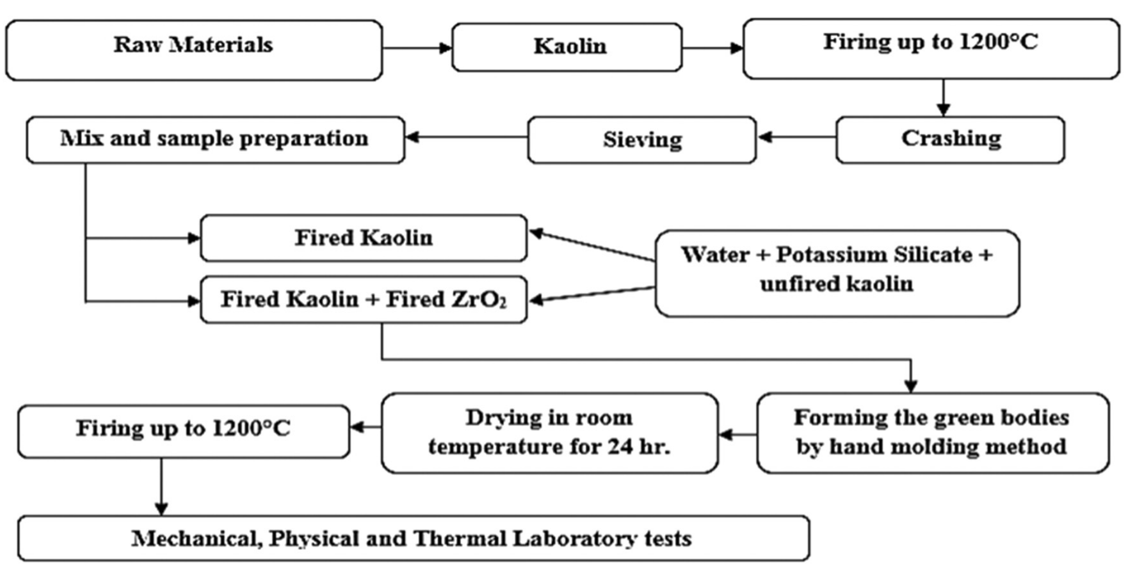


**Figure 1:** Block diagram of the present work.

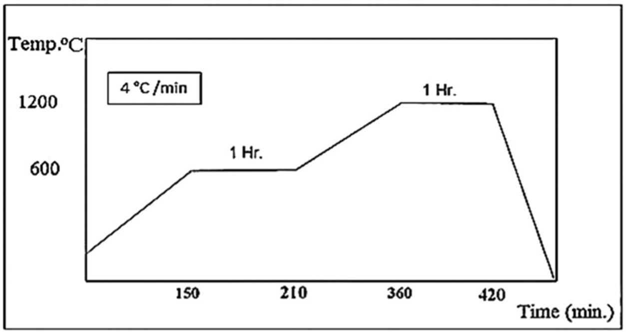


**Figure 2:** Firing program of the present work.

# 3 Procedure for testing

## 3.1 Bulk density and apparent porosity

The specimens were immersed in water to measure the bulk density and the apparent porosity. Eqs. (1) and (2) were applied on cylindrical specimens with the dimensions of 20 mm × 10 mm in accordance with ASTM C20 [18]:

$$\text{Bulk density} = D/W - S, \tag{1}$$

$$\text{Apparent porosity} = [(W - D)/(W - S)] \times 100, \tag{2}$$

where $D$ denotes dry weight (g), $W$ denotes saturated weight (g), and $S$ denotes suspended weight (g).

## 3.2 Linear shrinkage

Clay additives are the primary cause of mass loss in specimens during firing. Kaolinite loses its chemical water, organic impurities, and other substances during the initial heating process. A Vernier calliper was used to determine shrinkage by measuring the dimensions of the specimens before and after firing. The total losses of clay at 1,200°C were measured by Eq. (3) using cylindrical specimens in accordance with ASTM C326-03 [19].

$$\text{Linear shrinkage} = \frac{L_\circ - L}{L_\circ} \times 100\%, \tag{3}$$

where ($L_o$) denotes the specimen's length before firing (mm) and ($L$) denotes the specimen's length after firing (mm).

**Table 2:** Chemical analysis of raw materials

| Oxide<br>Raw materials | L.O.I % | $K_2O$% | $Na_2O$% | MgO% | CaO% | $TiO_2$% | $Fe_2O$% | $Al_2O_3$% | $SiO_2$% |
|---|---|---|---|---|---|---|---|---|---|
| Kaolin | 12.3 | 0.23 | 0.2 | 0.61 | 2.5 | 1.08 | 1.65 | 31.82 | 49.64 |

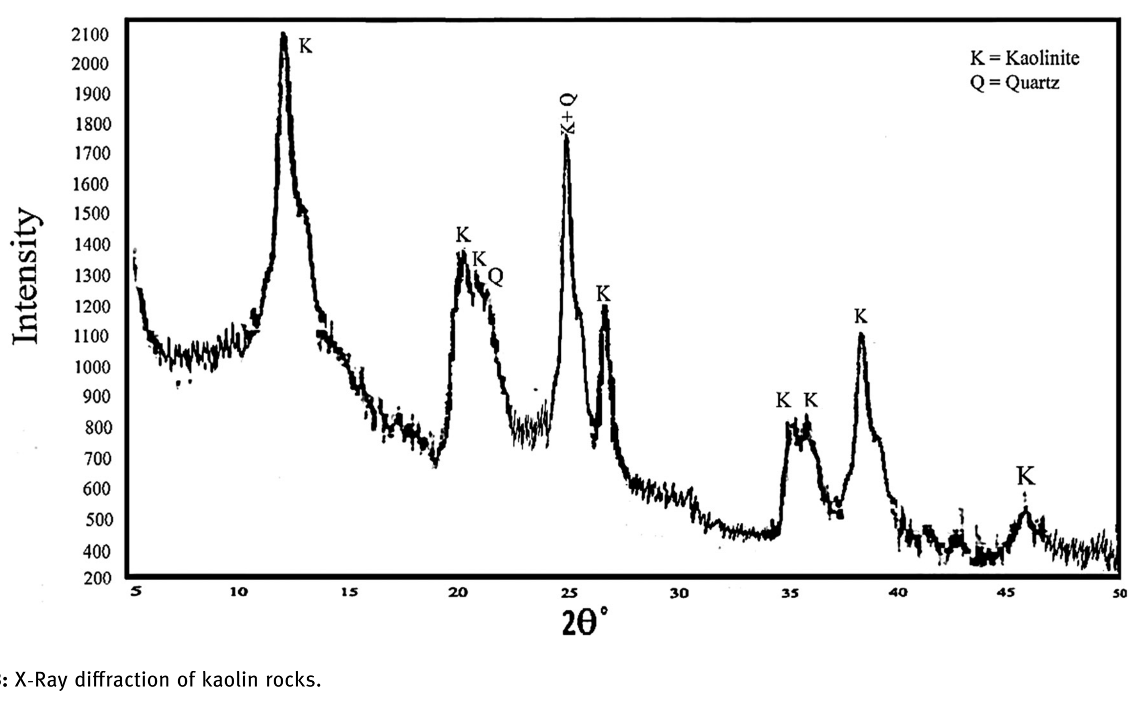


**Figure 3:** X-Ray diffraction of kaolin rocks.

### 3.3 Compressive strength

The compressive strength of cylindrical specimens was measured using Eq. (4) in accordance with ASTM C-773 [20].

$$\text{Compressive strength (MPa)} = \frac{F}{A}, \tag{4}$$

where $F$ is the applied load ($N$) and $A$ is the area under the load (mm$^2$).

### 3.4 Thermal shock

The resistance of thermal shock is typically determined by quenching the specimens from higher temperatures and calculating the strength as it decreases in comparison to room temperature. The specimens were heated to 500 and 1,000°C for 15 min before being rapidly quenched in ice-cold water at 0°C according to ASTM C1525 [21]. The compression strength measurement apparatus was used to determine the retained strength.

### 3.5 Thermal conductivity

Thermal conductivity was measured by adopting Lee's disc examination method. The device consists of a heater and three discs arranged with the test sample (S). The device is isolated from the outside environment by means of a glass container to ensure the accuracy of the results. The heater is equipped with a voltage that passes a current in a closed circuit, and the discs are heated directly on both sides of the heater. Then, the heat is transferred to the specimen and disc (A) at thermal equilibrium. The final temperatures are recorded, and by knowing the dimensions of the discs (A, B, and C) and the specimen (S), the thermal conductivity coefficient was calculated, and the amount of heat transferred (e) through the specimen (in W/m$^2$ K) was calculated from the following equation:

$$\begin{aligned} \mathrm{IV} = \pi D^2 \mathrm{e}(T_\mathrm{A} + T_\mathrm{B}) + 2\pi D e[d_\mathrm{A} T_\mathrm{A} + d_\mathrm{s}\left(\frac{1}{2}\right)(T_\mathrm{A} + T_\mathrm{B} \\ + d_\mathrm{B} T_\mathrm{B} + d_\mathrm{C} T_\mathrm{C}]). \end{aligned} \tag{5}$$

From (e), the thermal conductivity coefficient ($K$) was determined based on the equation which is as follows:

$$\begin{aligned} K \times (T_\mathrm{B} - T_\mathrm{A}/\mathrm{ds}) = e[T_\mathrm{A} + 2/D\ (d_\mathrm{A} + 1/4 d_\mathrm{s})\ T_\mathrm{A} \\ + 1/2 D d_\mathrm{s} T_\mathrm{B}]. \end{aligned} \tag{6}$$

where $I$ represents the current (0.25 A); $V$ represents the voltage (6 V); $T_\mathrm{A}$, $T_\mathrm{B}$, and $T_\mathrm{C}$ represent the final temperature ($K$) for A, B, and C discs, respectively, and $d_\mathrm{A}$, $d_\mathrm{B}$, $d_\mathrm{C}$, and $d_\mathrm{s}$ represent the disc and specimen thicknesses, respectively.

## 4 Results and discussion

### 4.1 Bulk density and apparent porosity

The increase in bulk density occurs due to the homogeneity and good compacting in the mix, which reduces porosity. The density is affected by the raw materials utilised in the mix, as well as the temperature at which they are fired. The findings revealed that there was an increase in density and decrease in porosity due to the formation of the mullite phase, which is denser than kaolin [22]. The porosity reduced exponentially with $ZrO_2$ addition. As the densification of fine powder is greater than the densification of coarse powder, the porosity declined gradually as particle size decreases, resulting in vacancy reduction when fine powder filled the vacancies within the coarse powder [23]. The results are shown in Figures 4 and 5.

### 4.2 Linear shrinkage

The size of the pores shrinks during firing, causing shrinkage in the specimen measurements. The amount of shrinkage in combination is determined by the raw

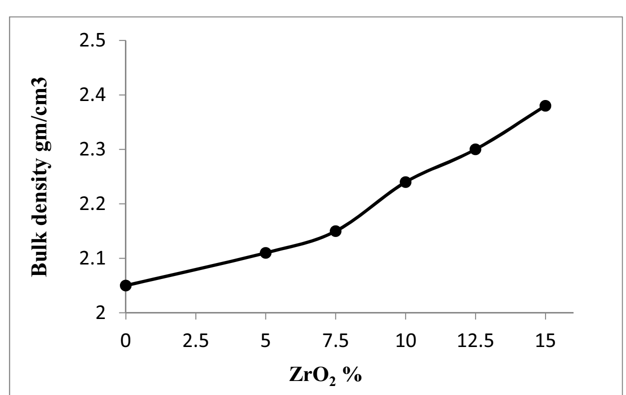


**Figure 4:** Bulk density for various $ZrO_2$ additions in refractory specimens.

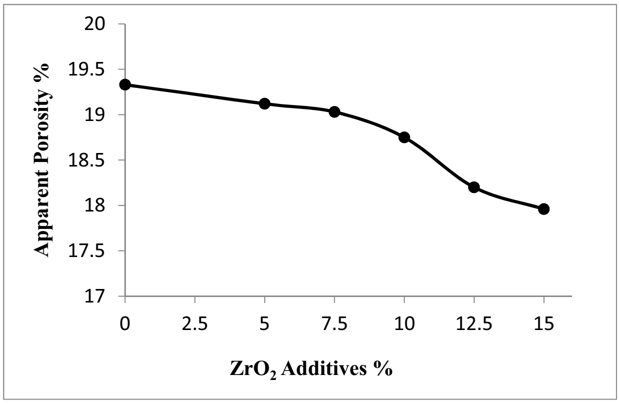


**Figure 5:** Apparent porosity for various $ZrO_2$ additions in refractory specimens.

materials utilised, particle size and distribution, as well as the firing temperature. Figure 6 shows a decrease in shrinkage values after firing due to mullite formation. The reaction of $Al_2O_3$ with $SiO_2$ produces the mullite phase. The addition of $ZrO_2$ reduced the linear shrinkage ratio. This addition reduced the proportion of raw materials involved in the preparation of refractories, hence reducing the proportion of the glass phase formed in refractory specimens and further reducing the linear shrinkage ratio. Furthermore, the high melting point of $ZrO_2$ has an important role in reducing the linear shrinkage of the prepared refractory specimens. The percentage of mullite increased, and the percentage of the glass phase formed from the kaolin ore decreased when firing with the addition of nano-$ZrO_2$ due to the small size of the nanopowder particles. A high percentage of the mullite phase and a low percentage of the glass phase decreased the percentage of linear shrinkage.

## 4.3 Compressive strength

The compressibility of mortars in refractory masonry linings of industrial furnaces is important for thermomechanical stability. The results of compressive strength for pure and $ZrO_2$ specimens are shown in Figure 7. The addition caused an increase in compressive strength because $ZrO_2$ increases the toughness and resistance of refractory specimens by increasing the density. A higher-density ceramic body has higher mechanical properties as a result of the pores forming weak areas in the ceramic body. On the other hand, $ZrO_2$ particles impede the movement of the microcracks in the refractory specimens under test, according to the particle reinforcement mechanism. Furthermore, sintering at high temperatures forms the liquid phase, which reduces porosity and closes pores, as well as increases particle cohesion and refractory material strength.

## 4.4 Thermal shock resistance

Thermal shock resistance was calculated by firing the specimens at 500 and 1,000°C and rapidly quenched in ice-cold water. Then, the compressive strength test was tested. The results are shown in Figure 8.

It is clear from the figure that the resistance decreased gradually with the increase in the temperature of the thermal shock for refractory specimens, and this stage is called the stage of elastic thermal behaviour, and it refers to the change in the size and shape of a solid object as the temperature of that object fluctuates, in which microcracks are generated. The prepared refractory specimens consist of several phases (*i.e.*, the mullite

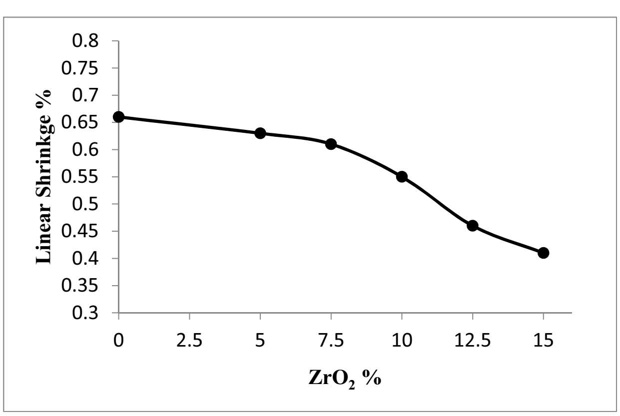


**Figure 6:** Linear shrinkage for various $ZrO_2$ additions in refractory specimens.

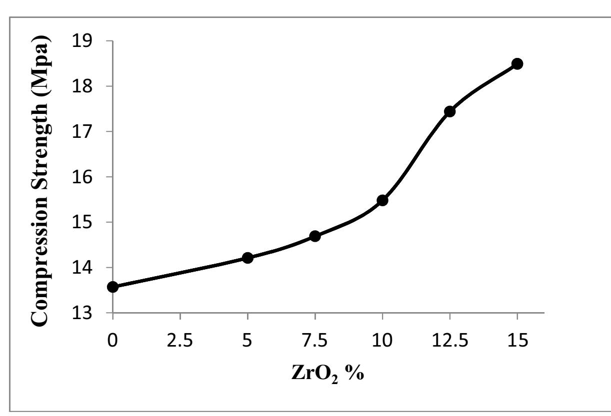


**Figure 7:** Compressive strength for various $ZrO_2$ additions in refractory specimens.

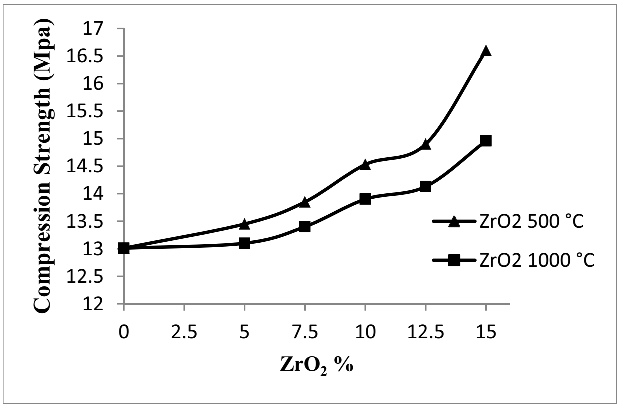


**Figure 8:** Compressive strength after thermal shock for various $ZrO_2$ additions in refractory specimens.

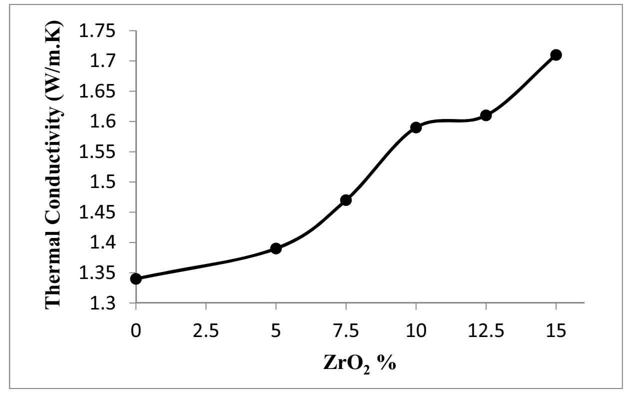


**Figure 10:** Thermal conductivity for various $ZrO_2$ additions in refractory specimens.

phase, $ZrO_2$, the liquid phase, and the porous phase) as a result of temperature changes and the difference in the coefficient of longitudinal thermal expansion for different phases, where thermal stresses localised and microcracks are produced, hence reducing the compressive strength. The glass phase contributes to the loss of strength during thermal shock, and the presence of kaolin can result in a reduction in temperature changes due to the low thermal shock resistance of kaolin. The added $ZrO_2$ nanoparticles inhibit the growth and movement of microcracks. The compressive strength values before and after quenching are shown in Figure 9.

### 4.5 Thermal conductivity

Thermal conductivity is influenced by porosity, which plays an important role in heat flow through refractories. Thermal conductivity decreases when porosity increases. The prepared mortar is a composite material consisting of several phases (*i.e.*, the mullite phase, nano-$ZrO_2$, the glass phase, and the porous phase). Figure 10 demonstrates the impact of added nano-$ZrO_2$ on the thermal conductivity of the prepared refractory specimens. It is clear from the figure that the addition of nano-$ZrO_2$ leads to an increase in the thermal conductivity value. The thermal conductivity continues to rise with the increase in the percentage of addition. The increase in thermal conductivity can be attributed to a reduction in porosity and a rise in density at high temperatures. This behaviour is caused by an increase in the sintering process, as well as crystal growth [24].

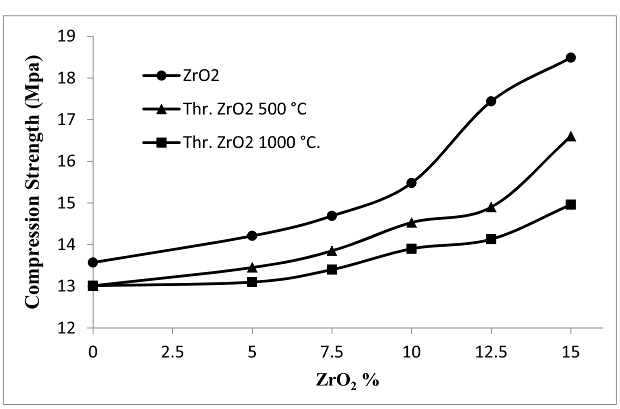


**Figure 9:** Compressive strength before and after quenching.

## 5 Conclusion

The thermal and mechanical stability of refractory mortar is very important, especially when used under elevated temperatures. Based on the experimental work and the conducted tests on the prepared refractory mortar, the addition of partially stabilised $ZrO_2$ is suitable for the production of refractory mortar because it leads to an increase in the bulk density and a decrease in both the apparent porosity and the linear shrinkage which also leads to increase the thermal conductivity. This increase in the density led to a significant improvement in the mechanical properties. After firing, the formation of the mullite phase improves the performance of the refractory mortar by providing strength and durability.

**Funding information:** The authors state no funding involved.

**Conflict of interest:** This is to inform you that there are no conflict of interest.

**Author contributions:** All authors have accepted responsibility for the entire content of this manuscript and approved its submission.

**Data availability statement:** The authors declare that this work has no data.

## References

[1] Schacht CA. Refractories hand book. New York: Marcel Dekker, Inc; 2004. p. 2.
[2] Boch P, Niepce JC. Ceramic materials. London: ISTE Ltd; 2007. p. 227–361.
[3] Singer F, Singer S. Industrial ceramic. Printed by photo lithography German; 1971. p. 988–1011.
[4] Tamar Agha MY. Internal report Geosurv, repo. No. (1840) Iraq; 1988.
[5] Tamar Agha MY. Internal report Geosurv, rep. No. (1899) Iraq; 1993.
[6] Bergaya F, Theng BK, Lagaly G. Clay science hand book. Amsterdam: Elsevier Science; 2006. p. 6, 20.
[7] Shackelford JF, Doremus RH. Ceramic and glass materials. New York: Springer; 2008. p. 27, 33, 111, 114.
[8] Ullmann F. Encyclopedia of chemical technology. 3rd ed. New York: John Wiley and Sons; 1982.
[9] Laming J. Refractory raw materials properties. Refract J. 1971;1(4):p6.
[10] Fue L, Khor KA, Lim JP. Processing microstructure and mechanical properties of yttria stabilizes zirconia reinforced hydroxyapatite coatings. Mater Sci Eng A. 2001;A316(1):46–51.
[11] Walker H. Handbook of refractories practice ceramic and glass materials. New York: Springer; 2008.
[12] Carter CB, Norton MG. Ceramic materials: Science and engineering. 2nd ed. New York: Springer; 2007.
[13] Weinberg AV, Goeuriot D, Poirier J, Varona C, Chaucherie X. Mullite–zirconia composite for the bonding phase of refractory bricks in hazardous waste incineration rotary kiln. J Eur Ceram Soc. 2021;41(1):995–1002.
[14] Brulin J, Blond E, de Bilbao E, Rekik A, Landreau M, Gasser A, et al. Methodology for brick/mortar interface strength characterization at high temperature. Constr Build Mater. 2020;265(30):120565.
[15] Karatas M, Benli A, Arslan F. The effects of kaolin and calcined kaolin on the durability and mechanical properties of self-compacting mortars subjected to high temperatures. Constr Build Mater. 2020;265(30):120300.
[16] Omar MH, Amin MH, Younis HA. Comparison of using nano-ZnO and nano-$Al_2O_3$ to improve the properties of prepared polymethyl methacrylate denture base. Appl Phys A. 2022;128:313.
[17] Zaidan SA, Omar MH. The effects of bauxite, metakaolin, and porosity on the thermal properties of prepared Iraqi clays refractory mortars. Appl Phys A. 2018;124:386.
[18] ASTM C20-00. Standard test methods for apparent porosity, water absorption, apparent specific gravity, and bulk density of burned refractory brick and shapes by boiling water; 2015.
[19] ASTM C1407 – 98. Standard practice for calculating areas, volume, and linear change of refractory shapes; 2016.
[20] ASTM C773-88. Standard test method for compressive (crushing) strength of fired whiteware materials; 2020.
[21] ASTM C1525. Standard test method for determination of thermal shock resistance for advanced ceramics by water quenching; 2018.
[22] Chima O, Nwoye C, Nnuka E. Enhancement of refractory properties of blended clay with groundnut shell and rice husk additives. Am J Eng Res. 2017;6(6):218–26.
[23] Chikwelu G, Onuegbu T, Ezeofor C, Akpomie K. Characterization of Mbaukwu Clay from Awka-South, Anambra State, Nigeria for industrial purposes. Pac J Sci Technol. 2018;19(1):251–56.
[24] Harith IJ, Hani MH. Study the bulk density, open porosity and coefficient of thermal conductivity of refractory mortar contains kaolin- metakolin-fire brick powder-SiC. Albahir J. 2019;10(19–20):57–66.